Anatomical and Functional Reflections of Vascular Changes in Retinitis Pigmentosa

Fatma Busra ALTAS (✉ fbusraaltas@gmail.com)
  Etlik City Hospital
Sibel DOGUIZI
  Ulucanlar Eye Training and Research Hospital
Elıf Gamze ONDER
  Elmadağ Dr. Hulusi Alatas State Hospital
Mehmet Ali SEKEROGLU
  Etlik City Hospital

Research Article

Additional Declarations: No competing interests reported.

Abstract

Purpose: Investigating the retinal vascular changes of retinitis pigmentosa patients in order to determine the anatomical, functional effects and the correlation between them, comparing them with healthy volunteers.

Methods: One eye of 25 RP cases and 25 healthy volunteers were included in this cross-sectional, comparative clinical study. After routine ophthalmological examination, pattern electroretinography (pERG) and optical coherence tomography angiography (OCTA) examinations were performed.

Results: Significant thinning was observed in all quadrants in the RP group (p<0.05 for all values) in foveal, parafoveal and perifoveal macular thickness measurement, In pERG analysis, prolonged P50 and N95 wave implicit time and decreased wave amplitudes were determined in patients with RP (p<0.05 for all values).

Superficial and deep capillary network vessel densities measured by OCTA were significantly lower in the RP group in all quadrants (p<0.001); FAZ parameters (area, perimeter and acircularity index (AI)) were higher in the RP group (p=0.042, p=0.001, p=0.014) and vascular density (FD) around FAZ was lower in the RP group compared to control group (p<0.001).

Conclusion: Vascular damage contributes to pathological process in RP patients. This vascular damage also affects the anatomical features of the retina. Using OCTA, a non-invasive imaging technique, we can estimate the stage, progression and prognosis of the disease in RP patients. İn non-advanced RP patients, the pERG waves are unsuitable for evaluation. Therefore pERG may not be suitable for functional evaluation in RP patients.

Introduction

Retinitis Pigmentosa is the most common hereditary retinal disease with an average prevalence of 1/4000 (1,2). It can be inherited autosomal dominant, autosomal recessive, X-linked recessive or sporadic (2). First complaint is difficulty in adaptation to the dark, followed by inability to see at night, scotomas in the midperiphery of the visual field, loss of peripheral visual field, tunnel vision, and loss of central vision (3). The age of onset and severity of symptoms vary according to inheritance pattern. Pigmentary bone speculum in the fundus, waxy optic disc, and thinning of the vessels are typical findings in ophthalmological examination (4).

Rod photoreceptors are mainly affected in RP (5). However, retinal pigment epithelium (RPE), cone receptors, ganglion cells, Muller cells, extracellular matrix and vascular structures are also affected by biochemical, mechanical and intercellular interaction pathways during pathological process of retina (6). Recent studies investigate the role of all these changes in the pathogenesis of the disease. Many studies emphasized the fact that the inner layers and vascular structure of the retina are affected in addition to

the outer layers in RP (7,8). Vascular thinning and disc pallor, which are included in three main features of the disease, also give an idea about vascular damage.

OCTA, which has an important clinical use in the diagnosis and follow-up of retinal diseases in recent years, has taken place in daily practice with the advantages of being non-invasive, being able to be applied in clinical conditions with no need of any contrast agent, being repeatable, and not having a time limit (9). Additionally, it enables to examine the microvascular structure of retina and choroid in layers and measure FAZ and macular thickness parameters.

Pattern ERG is an electrophysiological test that helps us to obtain information about the macula and optic nerve by evaluating the functions of ganglion cells (10). In pERG, there is three waves, two negative and one positive. The first negative wave is N35 that occurs at the 35th millisecond (ms). P50 is a large positive wave that occurs at 50-60 ms and is used to evaluate macular function. N95 is the third large negative wave that occurs at 90-100 ms and helps to evaluate the optic nerve response. An objective functional evaluation can be provided with pERG follow-up in RP patients having preserved central macular function and tubular vision (11).

In our study, we aim to evaluate vascular involvement and anatomical features of the macula by OCTA in RP; functional evaluation by pERG. Therefore, in addition to the current literature, we intent to examine the vascular changes in RP in more detail with OCTA, to better understand the clinical presentation of the disease, to make a more objective functional evaluation with pERG, and to make more accurate predictions about the prognosis of the disease.

MATERIALS AND METHODS

Design of the Study

One eye of 25 patients between 20–50 years-old with a definitive diagnosis of RP with characteristic clinical finding (night blindness), fundus (wax optic disc, bony specules, attenuation of retinal vessels) and full-field ERG (ffERG) measurements (decreased scotopic and photopic responses) and 25 healthy individuals who applied to Health Sciences University Ulucanlar Eye Training and Research Hospital between January 2019 and December 2019 were included in this cross-sectional, comparative clinical study.

Detailed biomicroscopic examination was performed for case and control groups. Anterior segment examination was performed with the Topcon SL-3G (Tokyo Optical Co. Ltd. Japan) device, dilated posterior segment examination with a 90 D (Volk Optical, Inc, USA) lens. Intraocular pressures were measured with Topcon CT–800 (Tokyo Optical 20 Co. Ltd. Japan) non-contact tonometry and refraction measurements with Huvitz HRK–7000A (Huvitz Co. Ltd. Korea). BCVA data was obtained using the LogMAR (Logarithm of the Minimum Angle of Resolution) chart.

Participants

History of previous ocular surgery or trauma; another optalmologic pathology like glaucoma, uveitis; pathologies that change the macular thickness measurement such as epiretinal membrane, cystoid macular edema, retinoschisis; pathologies that decrease the quality of the shooting such as cataract, vitreous opacity or nystagmus; co-morbid systemic disease affecting retinal microcirculation (diabetes mellitus, hypertension..etc); ±6 diopters spherical, > ±2 diopters cylindrical refractive error; history of amblyopia in any eye with anisometropia more than 3 diopters; history of drug use causing potential retinal toxicity or affecting test results; pupillary anomaly and anisocoria; lack of cooperation, using prosthetic devices or devices generating electromagnetic fields, syndromic and atypical RP cases and advanced stage RP with a BCVA less than 1.0 LogMAR were exclusion criterias.

pERG Measurements

Pattern ERG measurements were performed by the same technician in a room isolated from magnetic field and sound, using HK loop electrodes with a Metrovision Monpack One (Mon2014D, Metrovision, France) device with topical anesthesia and in accordance with ISCEV standards. Metrovision Monpack One device had an excitation LCD (Liquid crystal monitors) with feedback pattern (to eliminate luminance artifact of standard LCD monitors). pERG measurements were obtained without pupil dilation and with appropriate refractive correction if necessary. After electrode placement, pERG was recorded while participant looking at the fixation point in the middle of the moving checkerboard patterns on the screen 1 meter ahead. The contrast between the black and white squares was 95% and the average brightness was 80 cd/m2. During the test, the technician checked the patients keeping eyes open and compliance with standarts. N35, P50 and N95 waves' amplitude and implicit time values were calculated automatically. Participants incompatible with pERG test, who couldn't fix adequately due to low visual acuity, and with similar conditions causing less reliable wave pattern were excluded from the study.

OCTA Measurements

Same experienced technician performed OCTA (AngioVue, RTVue XR Avanti SD-OCT, Optovue, Fremont, CA, USA) after pupillary dilation with 1% tropicamide after pERG measurement, at the similar time zone (14.00–15.00) and environmental conditions. 6x6 mm image option was preferred for macular analysis using software (Optovue, Version 2015.100.0.35), Patients with low image quality (signal strength index < 6/10), low vision, limited fixation and artifacts affecting structural imaging were excluded from the study.

Measurements of fovea, parafovea, and perifovea capillary network vessel density (%) corresponding to macular areas of the superficial and deep capillary plexus were recorded in accordance with early treatment diabetic retinopathy study (ETDRS) grid pattern (1mm, 3mm, and 6 mm) (Fig. 1). Segmentation was performed automatically by the software confining SCP between inner limiting membrane and inner plexiform layer; and DCP between inner plexiform and outer plexiform layers. Foveal avascular zone (FAZ, mm2), perimeter (FAZ circumference, mm), acircularity (circularity) index (AI = FAZ circumference/perimeter), FAZ 300 micron circumference vessel density (FD, %) were measured automatically (Fig. 2). Quickvue module of OCTA was used to determine central macular thickness

measurement for all retinal thickness parameters matching the ETDRS grid model. The distance between the ILM and RPE layers was automatically mapped with centralizing the fovea (Fig. 2).

Statistical Analysis

Statistical analysis was performed using IBM SPSS (Statistical Package for Social Sciences) Statistics for Windows, version 22.0 (SPSS Inc, Chicago, IL). Descriptive statistics were presented as mean ± SD (minimum-maximum), frequency distribution, and percentage. Pearson Chi-Square Test was used to evaluate categorical variables. Distribution pattern of variables was tested using visual (histogram and probability graphs) and analytical methods (Shapira-Wilk Test). For normally distributed variables, student's T Test, for non-normally distributed variables, Mann-Whitney U Test was used to detect any significant difference between two independent groups. Correlations between variables were tested by Spearman correlation analysis. Correlation coefficient was defined as 'weak' between 0-0.25, as 'moderate' between 0.26−0.50, as 'strong' between 0.51−0.75, as 'very strong' between 0-76-1.00. The P values less than 0.05 were considered to be statistically significant.

RESULTS

The distribution of age, gender, BCVA and intraocular pressure between study groups (retinitis pigmentosa and control groups) is presented in Table 1. While the BCVA in terms of LogMAR of RP patients was significantly lower than the control group ($p < 0.001$), no statistically significant difference was found between two groups in terms of age, gender and intraocular pressure ($p > 0.05$) (Table 1).

Table 1
Distribution of age, gender, BCVA and intraocular pressure among study groups

	Retinitis Pigmentosia (n = 25)	Control (n = 25)	p
Age (year)	37.9 ± 9.2 (25−56)	33.6 ± 8.5 (23−50)	0.107[a]
Sex			
Male	15 (60.0)	14 (56.0)	0.774[b]
Female	10 (40.0)	11 (44.0)	
Visual Acuity (LogMAR)	0.25 ± 0.15 (0-0.52)	0.02 ± 0.04 (0-0.10)	< 0.001[a]**
İntraocular pressure (mmHg)	16.3 ± 2.2 (12−21)	15.6 ± 2.3 (11−20)	0.291[c]
Categorical variables were presented as "number (percent of column)" and continuous variables as "mean ± standard deviation (minimum-maximum)", n: Number of eye; [a]Mann-Whitney U Test; [b]Ki-Kare Test; [c]Student's T Test; *p < 0.05; **p < 0.01			

Significant thinning of macular thickness in accordance with ETDRS grid model was observed in RP group compared to control group in foveal, parafoveal and perifoveal four quadrants ($p < 0.05$ for all

values) (Table 2).

Table 2
Distribution of macular thickness measurements among study groups

Macular Thickness(μm)	Retinitis Pigmentosia (n = 25)	Control (n = 25)	p^a
	mean ± SD (min-max)	mean ± SD (min-max)	
Fovea	241.4 ± 36.1 (154−299)	260.1 ± 15.9 (220−287)	0.024*
Parafovea			
Superior	269.6 ± 30.5 (221−336)	343.3 ± 16.2 (310−370)	< 0.001**
Nasal	262.8 ± 33.2 (207−345)	337.4 ± 15.0 (305−369)	< 0.001**
İnferior	265.2 ± 30.0 (210−335)	341.2 ± 15.8 (299−364)	< 0.001**
Temporal	265.1 ± 30.1 (209−341)	333.0 ± 15.7 (295−362)	< 0.001**
Perifovea			
Superior	224.5 ± 32.0 (169−289)	301.9 ± 18.8 (260−327)	< 0.001**
Nasal	222.2 ± 33.1 (159−282)	307.6 ± 21.3 (266−338)	< 0.001**
İnferior	220.6 ± 32.2 (165−280)	292.4 ± 15.2 (260−315)	< 0.001**
Temporal	222.2 ± 33.3 (162−289)	297.3 ± 19.7 (250−343)	< 0.001**

μm: mikrometer, n: Number of eye; mean: Mean; SD: Standart deviation; [a]Student's T Test; *p < 0.05; **p < 0.01

N35, P50 and N95 waves implicit times were significantly higher in RP group than control group. On the other hand, P50 and N95 waves amplitudes were significantly lower in RP group than control group (p < 0.05) (Table 3).

Table 3
Distribution of pERG parameters among study groups

PERG		Retinitis Pigmentosia (n = 25)	Control (n = 25)	p^a
		ort ± SD (min;maks)	ort ± SD (min;maks)	
N35	Amplitude (μV)	-0.14 ± 0.41 (-0.8;1.0)	-0.40 ± 0.76 (-2.3;1.0)	0.332
	İmplicide time(ms)	36.8 ± 3.1 (31.8;46.0)	31.4 ± 3.5 (26.9;39.8)	**< 0.001****
P50	Amplitude (μV)	0.81 ± 0.82 (-0.1;3.6)	3.26 ± 0.63 (2.1;5.2)	**< 0.001****
	İmplicide time(ms)	59.4 ± 8.5 (45.1;79.6)	51.0 ± 2.4 (47.6;56.6)	**< 0.001****
N95	Amplitude (μV)	-0.90 ± 0.77 (-3.3;0.1)	-5.29 ± 1.05 (-6.8;-2.3)	**< 0.001****
	İmplicide time (ms)	106.4 ± 13.7 (91.1;150.0)	92.5 ± 3.3 (86.4;97.5)	**< 0.001****

ms: millisecond, μV: microvolt, n: Number of eye; mean: Mean; SD: Standart deviation; [a]Mann-Whitney U Test; *p < 0.05; **p < 0.01

In OCTA measurements, FAZ parameters and SCP, DCP vessel density (%) between two groups are presented in Table 4. Some FAZ parameters including area, perimeter and AI measurements were statistically significantly higher in RP group (p = 0.042, p = 0.001, p = 0.014, respectively). On the contrary, FD value was lower in RP group than control group (p < 0.001). SCP and DCP vessel densities were significantly lower in all quadrants and layers in RP group compared to control group (p < 0.001 for all values).

Table 4
Distribution of FAZ parameters and vessel density measurements among study groups

		Retinitis Pigmentosia (n = 25)	Control (n = 25)	p^a
		mean ± SD (min-max)	mean ± SD (min-max)	
FAZ	Area (mm^2)	0.30 ± 0.11 (0.20−0.61)	0.24 ± 0.10 (0.11−0.45)	0.042*
	PERIMETER	2.26 ± 0.40 (1.71−3.21)	1.82 ± 0.38 (1.36−2.61)	0.001**
	AI	1.15 ± 0.07 (1.09−1.38)	1.10 ± 0.05 (1.01−1.18)	0.014*
	FD	44.0 ± 6.4 (27.8−53.0)	53.7 ± 5.3 (44.3−61.7)	< 0.001**
SCP (%)	Whole Area	42.7 ± 4.6 (33.9−55.2)	50.9 ± 3.8 (40.6−56.7)	< 0.001**
	Superior Half	42.6 ± 4.7 (34.9−54.6)	50.7 ± 3.8 (41.7−57.2)	< 0.001**
	Inferior Half	43.0 ± 5.0 (33.2−55.8)	51.0 ± 4.0 (39.5−56.1)	< 0.001**
	Fovea	6.8 ± 5.0 (0.9−21.2)	20.4 ± 4.0 (12.6−27.6)	< 0.001**
	ParaFovea	36.6 ± 5.5 (26.4−47.7)	52.4 ± 4.7 (40.8−58.4)	< 0.001**
	ParaFovea Superior Half	35.5 ± 6.1 (24.6−49.0)	52.4 ± 4.6 (40.6−58.5)	< 0.001**
	ParaFovea Inferior Half	37.8 ± 6.1 (24.4−47.6)	52.4 ± 4.9 (41.0-58.3)	< 0.001**
	ParaFovea Temporal	35.4 ± 10.1 (18.2−55.6)	51.9 ± 4.8 (41.3−57.5)	< 0.001**
	ParaFovea Superior	37.6 ± 8.2 (24.8−52.1)	53.1 ± 5.4 (36.2−60.1)	< 0.001**
	ParaFovea Nasal	33.0 ± 7.4 (20.7−50.7)	52.1 ± 4.5 (40.1−56.8)	< 0.001**
	ParaFovea Inferior	40.4 ± 7.8 (27.3−52.9)	52.6 ± 5.2 (41.9−59.7)	< 0.001**
	PeriFovea	44.6 ± 4.4 (34.8−49.5)	51.5 ± 4.0 (40.6−58.8)	< 0.001**

		Retinitis Pigmentosia (n = 25)	Control (n = 25)	p^a
		mean ± SD (min-max)	mean ± SD (min-max)	
	PeriFovea Superior Half	44.4 ± 4.2 (36.0-49.3)	51.0 ± 4.0 (41.8–58.8)	< 0.001**
	PeriFovea Inferior Half	44.9 ± 5.3 (32.4–50.7)	52.0 ± 4.2 (39.4–58.8)	< 0.001**
	PeriFovea Temporal	40.5 ± 5.3 (30.8–49.5)	46.7 ± 5.1 (32.6–52.9)	< 0.001**
	PeriFovea Superior	43.6 ± 4.1 (33.5–49.5)	50.6 ± 4.6 (41.4–60.8)	< 0.001**
	PeriFovea Nasal	49.1 ± 4.5 (39.3–55.7)	55.8 ± 3.0 (47.5–61.4)	< 0.001**
	PeriFovea Inferior	45.3 ± 6.8 (28.8–54.7)	53.3 ± 4.2 (41.2–60.2)	< 0.001**
DCP(%)	Whole Area	41.2 ± 4.1 (34.8–48.9)	49.6 ± 5.5 (38.7–56.4)	< 0.001**
	Superior Half	41.4 ± 4.2 (34.9–50.1)	50.2 ± 5.8 (38.6–56.5)	< 0.001**
	Inferior Half	41.0 ± 4.2 (33.2–48.4)	49.0 ± 5.5 (37.9–56.2)	< 0.001**
	Fovea	23.6 ± 5.4 (2.5–31.6)	40.3 ± 5.2 (30.0-47.4)	< 0.001**
	ParaFovea	44.2 ± 6.0 (32.9–56.3)	55.5 ± 3.4 (48.4–60.4)	< 0.001**
	ParaFovea Superior Half	44.4 ± 6.6 (29.0-56.4)	55.0 ± 4.5 (40.3–60.0)	< 0.001**
	ParaFovea Inferior Half	44.1 ± 5.9 (33.0-56.2)	55.2 ± 3.6 (47.7–60.6)	< 0.001**
	ParaFovea Temporal	44.2 ± 7.5 (23.0-54.8)	56.5 ± 3.0 (50.2–60.8)	< 0.001**
	ParaFovea Superior	45.4 ± 6.5 (34.5–59.2)	54.9 ± 4.0 (48.1–60.0)	< 0.001**
	ParaFovea Nasal	43.8 ± 6.8 (32.1–55.2)	56.8 ± 3.4 (50.3–61.3)	< 0.001**
	ParaFovea Inferior	43.9 ± 6.6 (26.7–56.3)	53.7 ± 4.3 (44.3–60.2)	< 0.001**

	Retinitis Pigmentosia (n = 25)	Control (n = 25)	p^a
	mean ± SD (min-max)	mean ± SD (min-max)	
PeriFovea	42.3 ± 4.4 (36.1−50)	50.7 ± 6.3 (38.1−58.4)	< 0.001**
PeriFovea Superior Half	42.8 ± 4.8 (36.0-51.1)	51.2 ± 6.5 (38.0-58.3)	< 0.001**
PeriFovea Inferior Half	42.2 ± 4.5 (36.0-50.6)	50.2 ± 6.5 (37.4−58.5)	< 0.001**
PeriFovea Temporal	39.7 ± 5.3 (31.5−50.3)	54.2 ± 5.2 (44.5−60.1)	< 0.001**
PeriFovea Superior	41.7 ± 5.2 (32.1−49.1)	49.3 ± 7.8 (33.8−57.9)	< 0.001**
PeriFovea Nasal	46.1 ± 4.2 (41.1−53.8)	49.9 ± 6.5 (36.5−57.1)	0.005**
PeriFovea Inferior	41.4 ± 5.0 (31.2−50.0)	49.4 ± 7.1 (36.5−58.7)	< 0.001**
n: Number of eye; mean: Mean; SD: Standart deviation; [a]Mann-Whitney U Test; *p < 0.05; **p < 0.01			

There was no statistically significant correlation between BCVA and macular thickness, pERG values in all groups (for both, p > 0.05).

There was negative, moderate (r= -0.44, r= -0.46, -0.40, respectively) correlation between BCVA and the vessel density of DCP in mean parafovea, inferior half and inferior quadrant of the parafovea. Also, there was a negative, strong (r= -0.53) statistically significant correlation between BCVA and vessel density of DCP in parafoveal nasal quadrant in RP group (p < 0.05). No correlation was detected between BCVA and vessel density of DCP in other quadrants, SCP and FAZ parameters (Table 5).

Table 5
The relationship between BCVA and FAZ parameters and vessel density measurements among study groups

| | | Visual Acuity (LogMAR) | | | |
| | | Retinitis Pigmentosia (n = 25) | | Control (n = 25) | |
		R	P	r	p
FAZ	Area (mm^2)	-0.021	0.922	-0.061	0.773
	PERIMETER	0.093	0.659	0.030	0.885
	AI	-0.039	0.852	0.306	0.136
	FD	-0.072	0.732	0.015	0.943
SCP(%)	Whole Area	-0.132	0.531	0.349	0.087
	Superior Half	-0.066	0.753	0.334	0.102
	Inferior Half	-0.050	0.813	0.349	0.087
	Fovea	-0.004	0.983	-0.106	0.613
	ParaFovea	0.119	0.570	0.243	0.242
	ParaFovea Superior Half	0.035	0.870	0.243	0.242
	ParaFovea Inferior Half	0.152	0.467	0.243	0.242
	ParaFovea Temporal	-0.025	0.904	0.076	0.718
	ParaFovea Superior	0.084	0.688	0.380	0.061
	ParaFovea Nasal	-0.149	0.477	-0.076	0.717
	ParaFovea Inferior	0.211	0.311	0.243	0.242
	PeriFovea	-0.268	0.196	0.334	0.102
	PeriFovea Superior Half	-0.245	0.238	0.344	0.093
	PeriFovea Inferior Half	-0.106	0.613	0.349	0.087
	PeriFovea Temporal	-0.026	0.903	0.349	0.087
	PeriFovea Superior	-0.308	0.135	0.258	0.212
	PeriFovea Nasal	-0.277	0.179	0.334	0.102
	PeriFovea Inferior	-0.101	0.631	0.334	0.102
DCP(%)	Whole Area	-0.289	0.161	-0.236	0.256
	Superior Half	-0.226	0.277	-0.182	0.383

	Visual Acuity (LogMAR)			
	Retinitis Pigmentosia (n = 25)		Control (n = 25)	
	R	P	r	p
Inferior Half	-0.317	0.123	-0.274	0.185
Fovea	0.033	0.877	-0.182	0.383
ParaFovea	-0.436	**0.030***	-0.091	0.665
ParaFovea Superior Half	-0.390	0.054	-0.015	0.942
ParaFovea Inferior Half	-0.464	**0.019***	-0.061	0.773
ParaFovea Temporal	-0.338	0.099	-0.304	0.140
ParaFovea Superior	-0.330	0.107	0.046	0.829
ParaFovea Nasal	-0.533	**0.006****	-0.106	0.612
ParaFovea Inferior	-0.404	**0.045***	0.076	0.718
PeriFovea	-0.221	0.289	-0.198	0.344
PeriFovea Superior Half	-0.145	0.490	-0.152	0.468
PeriFovea Inferior Half	-0.244	0.240	-0.258	0.212
PeriFovea Temporal	-0.293	0.155	-0.106	0.612
PeriFovea Superior	-0.216	0.300	-0.213	0.307
PeriFovea Nasal	-0.288	0.162	-0.228	0.273
PeriFovea Inferior	-0.290	0.159	-0.258	0.212
n: Number of eye; r: Spearman correlation coefficient; *p < 0.05; **p < 0.01				

In RP group, there was a negative, strong (r= -0.65) correlation between CMT and FAZ area; also a negative, moderate, statistically significant correlation between CMT and FAZ perimeter (r= -0.47) (p < 0.05); no statistically significant correlation between other FAZ parameters and macular thickness (p > 0.05).

DISCUSSION

We detected a decrease in superficial and deep capillary network vessel densities of the retina, an increase in the FAZ parameters and a thinning of the macular thickness in detailed anatomical analysis performed by OCTA, a non-invasive imaging technique, in RP patients. Also, pERG waves were unsuitable for functional evaluation, even in non-advanced RP patients.

Optical Coherens Tomography Angiography in Retinitis Pigmentosa

Vascular Changes

Optical coherence tomography angiography is a non-invasive, repetable technique that allows visualization of retinal and choroidal vessels without contrast material. Unlike FFA; It is an important advantage that it enables to image the DCP and choriocapillaris (CC) layer. FAZ and related parameters can be measured more objectively and reliably with OCTA (12).

Attenuation of retinal vessels is an important finding of RP (13). Thinning of retina-choroidal vessels and decrease in blood flow plays a prominent role especially in the loss of macular function (14–17). Toto et al. found a significant decrease in retinal and choriocapillaris vessel density in RP patients, and hypothesized that decrease effects macular function adversely, just like the ganglion cell complex (14). Jaureguj et al. found a decrease in SCP and DCP vessel densities and an increase in the FAZ. Also, they suggested that it is possible to get information about the progression of disease according to this data (16).

The cause of vascular attenuation in retinitis pigmentosa is still unclear. One of the hypotheses is that the outer retinal layers' oxygen requirement decreases after photoreceptor cell death. Thus, inner retina gets more oxygen supply, hyperoxic state, resulting in vasoconstriction (18–20).

Another hypothesis is that the outer layers get thinner after photoreceptor cell death causing extracellular matrix thickening. Thicker extracellular matrix surrounds the RPEs migrating to vessel periphery and results in deterioration in the vascular structure (21, 21). One more hypothesis is that synaptic input loss as a result of photoreceptor cell death causes reduction in trophic factors and vascular remodeling with disrupted metabolism of the inner retinal layers. Consequently, blood flow to the remaining retina is reduced (23). The common result of these three hypotheses is that vascular changes develop secondary to photoreceptor cell death. However, studies of mouse models with RP indicate that photoreceptor damage is prevented by retinal vessels' modulation (23). So, relationship between photoreceptor and vascular damage is intertwined and continues by feeding each other.

In our study, we detected a significant decrease in vessel density of SCP and DCP in all quadrants of foveal, parafoveal and perifoveal areas in RP group (Fig. 3). There was a statistically significant and moderate-strong negative correlation between BCVA and especially DCP vessel density decrease in the parafoveal area in the scope of OCTA vascular density changes, Battaglia et al detected by OCTA that SCP and DCP vascular densities decreased in RP group compared to control group. They claimed that the vascular disorder in RP is mostly in DCP (15). Likely, Rabiolo et al reported that vascular disorders are concentrated mostly in DCP, and SCP is not usually involved in RP (25). The facts that photoreceptors are primarily affected and DCP plays major role in the nutrition of the outer and middle layers of the retina, explain how DCP changes detected in our study effect BCVA.

Macular Thickness Change

The facts that ganglion cell layer is the thickest in the macula and cone photoreceptors are especially dense in the foveola, make macular thickness measurement important in terms of giving information about ganglion cell structure and photoreceptors. There can be thinner macula because of atrophy, on the contarary increase in thickness due to ERM may also be detected in RP patients. Macular thickness can also be detected as normal in early period RPs with no cone and RPE destruction (26).

In our study, we examined macular thickness as foveal, parafoveal four quadrants and perifoveal four quadrants according to the ETDRS grid model. In all quadrants, macular thickness was statistically significantly thinner than in RP group compared to control group. The mean CMT was 241.4 ± 36.1μm in RP group. The study of Lupo et al in which 118 eyes of 59 RP patients were clasified into four groups according to their OCT findings, indicated no macular thickness change on OCT in 36 eyes of first group. The mean age of the first group was 33.5 ± 7.4 years, with a mean BCVA of 0.95 ± 0.07 and a mean central macular thickness (CMB) of 256.3 ± 9.14 μm. The second and third groups include patients with macular edema and vitromacular traction on OCT. In the fourth group in which 28 eyes with macular thinning on OCT included, the mean age was 52.1 ± 13.6; BCVA was 0.36 ± 0.15 and mean CMT was 174.2 ± 24.4μm. As a conclusion, retinal thinning was detected more frequently in older ages and was associated with low BCVA level in that study (27). The mean age, BCVA and CMT values of RP group in our study had similarity to the first group of patients in Lupo et al.'s study. Moschos et al. evaluated 66 eyes of 33 patients and reported the mean foveal thickness as 152.95 ± 38.00 μm (28). Likely, we determined that CMT was significantly thinner in RP patients compared to healthy individuals.

The correlation between BCVA and CMB was determined differently in different studies. This can be explained by the difference in mean visual acuities of the patients in different studies. The preserved structural and functional properties of the macula determine BCVA in RP. Kim et al. reported that CMT was directly related to low BCVA in 71 eyes with CMT of 200 μm or less in a study involving 128 RP patients. Accordingly, in patients with thinner CMT, photoreceptor density decreased and BCVA deteriorated regardless of the presence of the IS/OS band (29). In our study, the thinnest fovea was detected at 154 μm and the lowest BCVA was 0.52 logMAR. The mean CMT and BCVA in RP group were 241.4μm and 0.25 logMAR. We couldn't find a correlation between BCVA and CMT despite the fact that both mean values were statistically significantly lowerin RP group than control group, We attribute this to relatively thicker CMT and higher BCVA of RP patients in our study. We can reveal the correlation between BCVA and CMT in case of more patients with advanced RP in RP group.

Relationship Between Vascular And Anatomical Structure

We found a statistically significant increase in FAZ area, perimeter and AI, and a decrease in FD in the RP group. AI is a value (nearly) equal to 1 if the circumference of the FAZ is smooth like a circle. If the AI value moves away from 1, it indicates deviations in the circular shape of the FAZ, this may be a prioneer indicator of ischemia of FAZ. Similarly, de Carlo et al. showed that the intercapillary area increase, retinal thickness decrease and some FAZ abnormalities were detected by OCTA in diseases with progressive

photoreceptor and RPE damage such as RP and Stargardt (30). Also, Battaglia et al. found that FAZ was increased especially at the level of DCP in RP patients. They couldn't detect a significant difference in the FAZ area at the level of SCP (16). In addition, there was a significant correlation between FAZ and CMT leading to the fact that FAZ widens as CMT decreases. We presume that the decrease in CMT is caused by the damage of the inner layers as a result of ischemia due to vascular density decrease.

Decrease in vascular densities, enlargement of the FAZ area, and thinning of the CMT are structural indicators of vascular and anatomical damage in RP. We hope that the detection of vascular changes in RP with OCTA may contribute to predict the prognosis of the disease and follow-up.

pERG Features in Retinitis Pigmentosa

Retinitis pigmentosa patients constitute a heterogeneous group in terms of disease progress. Some patients lose central vision at early stages, some can preserve visual acuity for many years. Electrophysiological tests give objective results in evaluating the functions of retinal cells. Full-field ERG can be used in the diagnosis of disease even in very early stages without symptoms, but It is incapable of demonstrating preserved central vision in patients with advanced RP. Multifocal ERG show loss of central cone function, but even patients with high BCVA may have irregular areas with faint responses. pERG is an objective test used to detect macular function. It reflects the functions of the inner retinal layers, especially ganglion cells (31). Nerve fiber atrophy occurs with transneural degeneration of ganglion cells as a result of photoreceptor destruction in RP (32, 33). Especially the P50 wave in pERG measurement that shows the macular function, may be useful in early detection of the macular damage in RP. Some patients with rod-cone dystrophy may have normal pERG measurements inspite of not having measurable waves in ffERG (31). Like histological changes, pERG can also correlate with BCVA. However, waves couldn't emerge in pERG even in RP patients with high BCVA (34). In Zira Janaky et al.'s study including 106 eyes of 53 RP patients, pERG and VEP records were performed. The measurable waves were formed in pERG of only 17 patients, and they couldn't get a normal pERG response from any patient (35). Robson et al. investigated the relationship between the diameter of the hyperautofluorescent ring detected in FAF and the amplitude of the pERG P50 wave in 30 RP patients with BCVA of 20/30 and beter. There was a positive correlation between the amplitude of P50 wave and the diameter of the hyperautofluorescent ring. The amplitude of p50 wave increases as hyperautofluorescent ring widens. The degree of macular involvement can be determined in RP patients with pERG, and these findings can be confirmed with FAF (37), forwhy, the hyperautofluorescence ring in FAF gives information about healthy photoreceptors. As FAF shows the structural features of the macula, a functional evaluation with pERG can be performed and correlate with FAF results.

We found that the amplitudes of the P50 and N95 waves were decreased and the implicit times were prolonged in RP group. pERG waves were even undetectable in some patients (Fig. 4). In our study, pERG waves were quite faint inspite of having better BCVA and CMT. Also, we couldn't detect any correlation between BCVA and pERG. This findings made us think that pERG is useless to detect macular function in RP. This may also caused by the fact that the small changes because of very low pERG wave amplitudes

didn't make statistically significant differences due to limited number of patients. In conclusion, further studies with larger groups are needed to determine the use of pERG in RP.

Declarations

ACKNOWLEDGEMENTS

CONFLICT OF INTEREST

Authors declare no conflicts of interest.

FUNDING

AUTHOR CONTRIBUTION STATEMENT

All authors contributed to the study conception and design. Material preparation, data collection and analysis were performed by Fatma Busra ALTAS, Sibel DOGUIZI, Elif Gamze ONDER, Mehmet Ali SEKEROGLU.

CONSENT TO PARTICIPATE and ETHICS APPROVAL

Written informed consent was obtained from all participants and study was conducted in accordance with the ethical principles of Declaration of Helsinki.

Approval was received from the Ethics Committee of Health Sciences University Ankara Numune Training and Research Hospital. (Date:02.21.2019/ Number:E-19-2539)

CONSENT TO PUBLISH

The authors affirm that human research participants provided informed consent for publication of the images in Figures 1,2,3 and 4.

References

1. Hamel C (2006) Retinitis Pigmentosa. Orphanet J Rare Dis 1:40–52. doi: 10.1186/1750-1172-1-40

2. Rivolta C, Sharon D, DeAngelis MM, Dryja TP (2002) Retinitis pigmentosa and allied diseases: numerous diseases, genes, and inheritance patterns. Hum Mol Genet 11:1219–1227. doi: 10.1093/hmg/11.10.1219

3. Dyonne T, Hartong DT, Berson EL, Dryja TP (2006) Retinitis Pigmentosa. Lancet 368:1795–1809. doi: 10.1016/S0140-6736(06)69740-7

4. Zhang Q (2016) Retinitis Pigmentosa: Progress and Perspective. Asia Pac J Ophthalmol 5:265–271. doi: 10.1097/APO.0000000000000227

5. Milam AH, Li ZY, Fariss RN (1998) Histopathology of the human retina in retinitis pigmentosa. Prog Retin Eye Res 17:175–205. doi: 10.1016/s1350-9462(97)00012-8

6. Campochiaro PA, Mir TA (2018) The mechanism of cone cell death in Retinitis Pigmentosa. Prog. Retin. Eye Res 62:24–37. doi: 10.1016/j.preteyeres.2017.08.004

7. Falsini B, Anselmi GM, Marangoni D, et al (2011) Subfoveal choroidal blood flow and central retinal function in retinitis pigmentosa. Invest Ophthalmol Vis Sci 52:1064–1069. doi: 10.1167/iovs.10-5964

8. Iacono P, Battaglia PM, La Spina, C, Zerbini G, Bandello F (2017) Dynamic and static vessel analysis in patients with retinitis pigmentosa: A pilot study of vascular diameters and functionality. Retina 37:998–1002. doi: 10.1097/IAE.0000000000001301

9. Spaide RF, Klancnik JM Jr, Cooney MJ (2015) Retinal vascular layers imaged by fluorescein angiography and optical coherence tomography angiography. JAMA Ophthalmol 133:45–50. doi: 10.1001/jamaophthalmol.2014.3616

10. Bach M, Brigel GM, Hawlina M, et al (2013) ISCEV Standard for clinical pattern electroretinography (PERG): 2012 update. Doc Ophthalmol 126:1–7. doi: 10.1007/s10633-012-9353-y

11. Holder GE, Brigell MG, Hawlina M, Meigen T, Vaegan, Michael Bach (2001) The pattern electroretingram. In: Electrophysiologic testing in disorders of the retina, optic nerve and visual pathway. The Foundation of the American Academy of Ophthalmology, 197–235.

12. Lu Y, Simonett JM, Wang J, et al (2018) Evaluation of Automatically Quantified Foveal Avascular Zone Metrics for Diagnosis of Diabetic Retinopathy Using Optical Coherence Tomography Angiography. Invest Ophthalmol Vis Sci 59:2212–2221. doi: 10.1167/iovs.17-23498

13. Ma Y, Kawasaki R, Dobson LP, et al (2012) Quantitative analysis of retinal vessel attenuation in eyes with retinitis pigmentosa. Invest Ophthalmol Vis Sci 53:4306–4314. doi: 10.1167/iovs.11-8596

14. Toto L, Borrelli E, Mastropasqua R, et al (2016) Macular Features in Retinitis Pigmentosa: Correlations Among Ganglion Cell Complex Thickness Capillary Density and Macular Function. Invest Ophthalmol Vis Sci 57:6360–6366. doi: 10.1167/iovs.16-20544

15. Battaglia PM, Cicinelli MV, Rabiolo A, et al (2018) Vessel density analysis in patients with retinitis pigmentosa by means of optical coherence tomography angiography. Br J Ophthalmol 101:428–432. doi: 10.1136/bjophthalmol-2016-308925

16. Jauregui R, Park KS, Duong JK, Mahajan VB, Tsang SH (2018) Quantitative progression of retinitis pigmentosa by optical coherence tomography angiography. Sci Rep 8, 13130 doi: 10.1038/s41598-

018-31488-1

17. Mastropasqua R, D'Aloisio R, De Nicola C, et al (2020) Widefield Swept Source OCTA in Retinitis Pigmentosa. Diagnostics 10:50 doi: 10.3390/diagnostics10010050

18. Padnick-Silver L, Kang Derwent JJ, Giuliano E, Narfstrom K, Linsenmeier RA. Retinal oxygenation and oxygen metabolism in Abyssinian cats with a hereditary retinal degeneration. Invest Ophthalmol Vis Sci 47:3683–3689 doi: 10.1167/iovs.05-1284

19. Yu DY, Cringle SJ (2005) Retinal degeneration and local oxygen metabolism. Exp Eye Res 80:745–751. doi: 10.1016/j.exer.2005.01.018

20. Penn JS, Li S, Naash MI (2000) Ambient hypoxia reverses retinal vascular attenuation in a transgenic mouse model of autosomal dominant retinitis pigmentosa. Invest Ophthalmol Vis Sci 41:4007–4013.

21. Cellini M, Strobbe E, Gizzi C, Campos EC (2010) ET-1 plasma levels and ocular blood flow in retinitis pigmentosa. Can J Physiol Pharmacol 88:630–635. doi: 10.1139/Y10-036.

22. Li ZY, Possin DE, Milam AH. (1995)Histopathology of bone spicule pigmentation in retinitis pigmentosa. Ophthalmology 102: 805–816 doi: 10.1016/s0161-6420(95)30953-0.

23. Stone JL, Barlow WE, Humayun MS, de Juan E Jr, Milam AH. (1992) Morphometric analysis of macular photoreceptors and ganglion cells in retinas with retinitis pigmentosa. Arch Ophthalmol. 110:1634–1639 doi: 10.1001/archopht.1992.01080230134038.

24. Otani A, Dorrell MI, Kinder K, et al. (2004) Rescue of retinal degeneration by intravitreally injected adult bone marrow-derived lineage-negative hematopoietic stem cells. J Clin Invest. 114:765–774 doi: 10.1172/JCI21686.

25. Rabiolo A, et al. (2019) Vascular abnormalities in patient with retintis pigmentosa assessed with optical coherence tomography angiography. J Clin Med.

26. Yoon CK, Yu HG. (2013) The Structure-Function Relationship between Macular Morphology and Visual Function Analyzed by Optical Coherence Tomography in Retinitis Pigmentosa. J Ophthalmol. doi: 10.1155/2013/821460

27. Lupo S, Grenga PL, Vingolo EM. (2011) Fourier-domain optical coherence tomography and microperimetry findings in retinitis pigmentosa. Am J Ophthalmol. 151:106–111 doi: 10.1016/j.ajo.2010.07.026.

28. Moschos MM, Chatziralli IP, Verriopoulos G, Triglianos A, Ladas DS, Brouzas D. (2013) Correlation between optical coherence tomography and multifocal electroretinogram findings with visual acuity in retinitis pigmentosa. Clin Ophthalmol. 7:2073–2078 doi: 10.2147/OPTH.S50752.

29. Kim YJ, Soo GJ, Dong-Hoo L, Joo YL, June-Gone, Young HY. (2013) Invest Correlations between Spectral-Domain OCT Measure-ments and Visual Acuity in Cystoid Macular Edema Associated with Retinitis Pigmentosa Ophthalmol Vis Sci. 54:1303–1309 doi: 10.1167/iovs.12-10149.

30. de Carlo TE, Adhi M, Salz DA, Joseph T, et al. (2016) Analysis of Choroidal and Retinal Vasculature in Inherited Retinal Degenerations Using Optical Coherehnce Tomography angiography. Opthalmic Surg Lasers Imaging Retina. 47:120–127 doi: 10.3928/23258160-20160126-04.

31. Holder GE. (2001) Pattern electroretinography (PERG) and an integrated approach to visual pathway diagnosis. Progress in Retinal and Eye Research. 20:531–561 doi: 10.1016/s1350-9462(00)00030-6.

32. Newman NM, Stevens RA, Heckenlively JR. (1987) Nerve fibre layer loss in diseases of the outer retinal layer. Br JOphthalmol. 71:21–26 doi: 10.1136/bjo.71.1.21

33. Flannery JG, Farber DB, Bird AC, Bok D. (1989) Degenerativechanges in a retina affected with autosomal dominant retinitis pigmentosa. Invest Ophthalmol Vis Sci. 30:191–211

34. Popovic P, Jarc-Vidmar M, Hawlina M. (2005) Abnormal fundus autofluorescence in relation to retinal function in patients with retinitis pigmentosa. Graefes Arch Clin Exp Ophthalmol. 243:1018–1027 doi: 10.1007/s00417-005-1186-x.

35. Janaky M, Palffy A, Horvath G, Tuboly G, Benedek G.(2008) Pattern-reversal electroretinograms and visual evoked potentials in retinitis pigmentosa. Doc Ophthalmol. 117:27–36 doi: 10.1007/s10633-007-9099-0.

36. Robson AG, El-Amir A, Bailey C, et al. (2003) Pattern ERG Correlates of Abnormal Fundus Autofluorescence in Patients with Retinitis Pigmentosa and Normal Visual Acuity. Invest Ophthalmol Vis Sci. 44:3544–3550 1167/iovs.02-1278
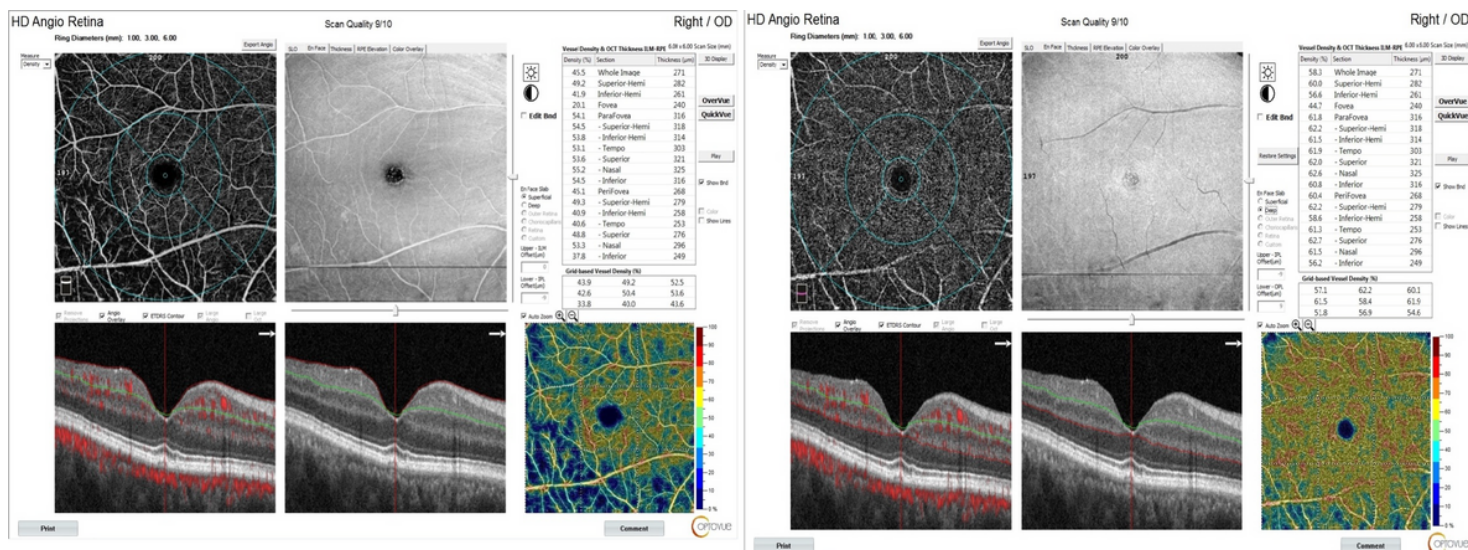
Figures

Figure 1

Superficial (left), deep (right) capillary plexus en-face and B-scan images and vessel density measurements in accordance with the ETDRS grid model
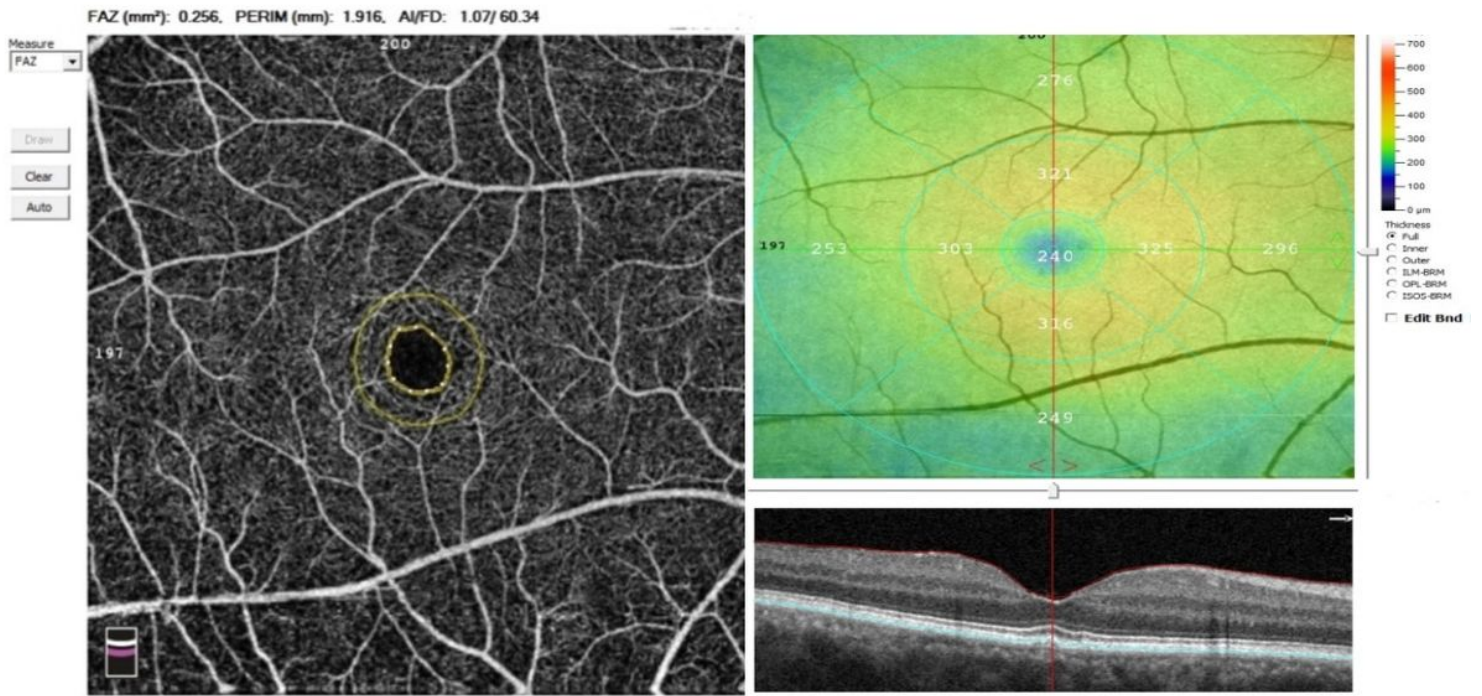
Figure 2

FAZ and FAZ related parameters (left), full-thickness retinal thickness measurements in accordance with the ETDRS grid (right)
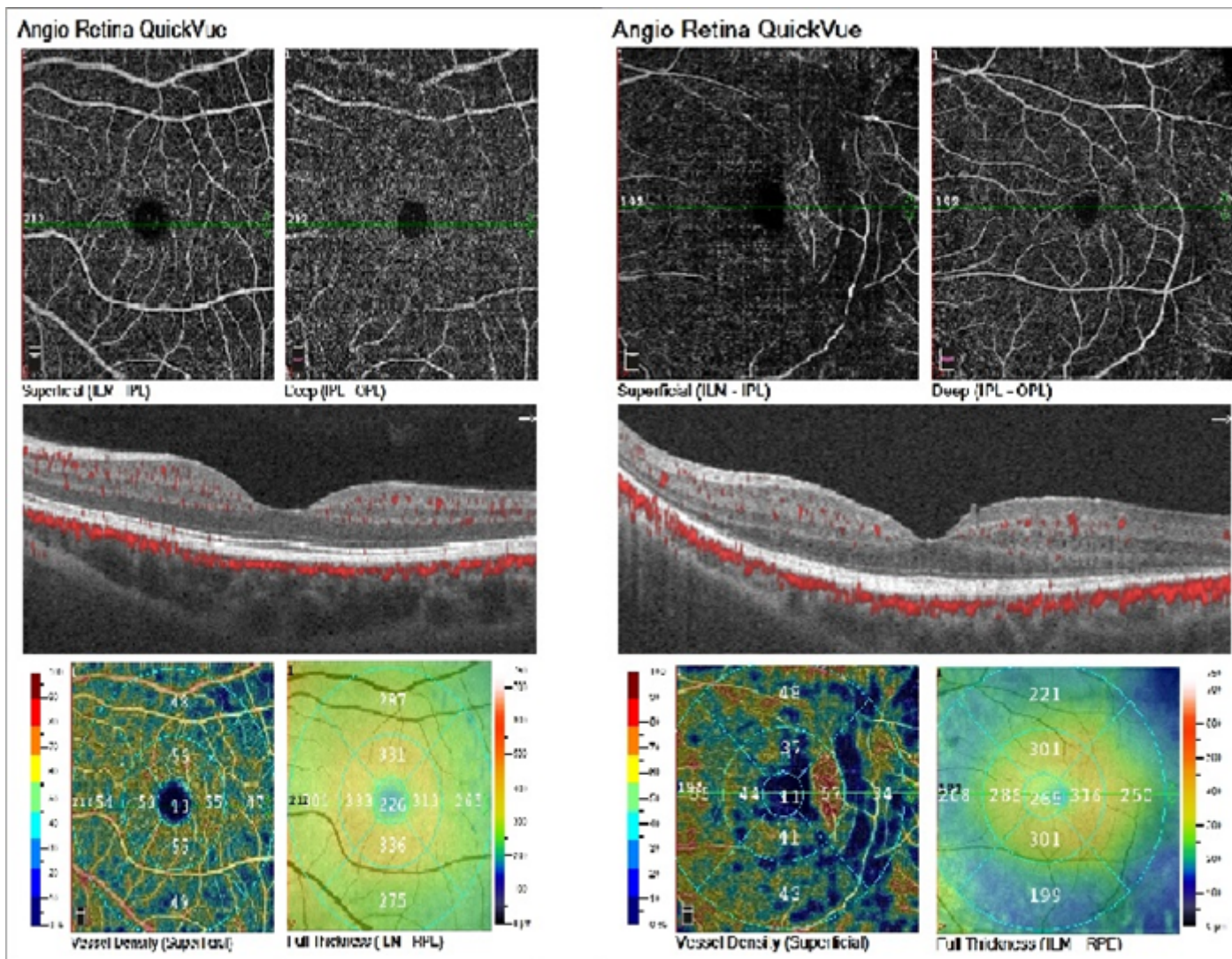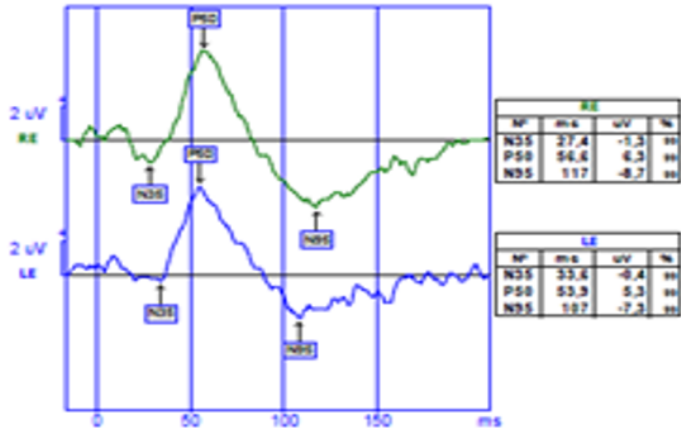
Figure 3

En-face sections of SCP and DCP and macular thickness measurement in OCTA (Images of a healthy volunteer on the right and a RP patient on the left)
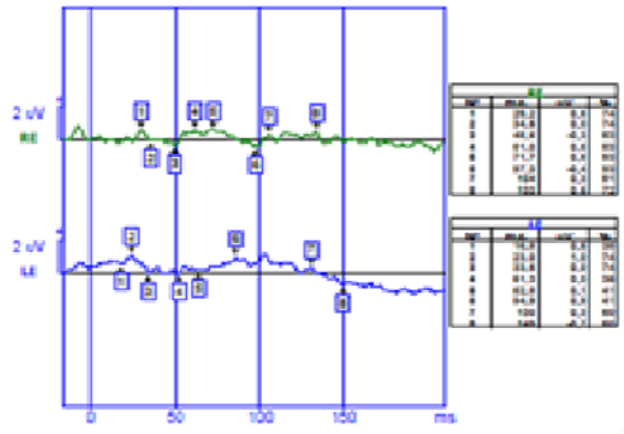
Figure 4

Our pERG analyzes' results (right from a healthy volunteer, left from a RP patient)